

## Negative magnetoresistance in ultrananocrystalline diamond: Strong or weak localization?

T. C. Choy and A. M. Stoneham

*London Centre for Nanotechnology, University College London, Gower Street, London WC1E 6BT, United Kingdom*

M. Ortuño<sup>a)</sup> and A. M. Somoza

*Departamento de Física-CIOyN, Universidad de Murcia, Murcia 30071, Spain*

(Received 24 September 2007; accepted 29 November 2007; published online 11 January 2008)

Electronic transport of ultrananocrystalline diamond involves the interplay between disorder, Anderson localization, and phase coherence. We show that variable range hopping explains many key features of the conductivity including the large low temperature negative magnetoresistance. Our numerical studies suggest two regimes where the (negative) magnetoresistance varies with magnetic field  $B$  such as  $B^2$  or  $B^{1/2}$ , respectively, depending on the ratio of the cyclotron orbital radius and the hopping distance. This agrees with experiment, which also points to the expected  $T^{-1/2}$  temperature dependence of the hopping distance at the critical field. © 2008 American Institute of Physics. [DOI: 10.1063/1.2826542]

The next generation of rugged, fast, higher voltage electronic devices presents major challenges to Si and even to SiC technologies. Diamondlike materials offer opportunities,<sup>1,2</sup> leading to many recent studies of ultrananocrystalline diamond.<sup>3</sup> Ultrananocrystalline diamond (UNCD) comprises ultrasmall diamonds, a few nanometers across with mainly  $sp^3$  bonding, embedded in an intergranular carbon that is largely  $sp^2$  bonded and almost certainly amorphous. We need to identify several key length scales. One will be associated with the nanostructure, typically the diameter ( $d \approx 2\text{--}20$  nm) of the nanodiamond particles. Another length scale will be the electron mean free path, or specifically  $L_\phi$ , the characteristic length of coherent diffusion. Its lower limit  $d_{\text{imp}}$  is a few angstroms, of the order of impurity spacing. A third length is the localization length, related to the size of the localized states which is short (of the order of  $d$  for strong localization). Finally, we have the quantum cyclotron radius,  $\ell_B = (\hbar/eB)^{1/2} \approx 26 \text{ nm}/B^{1/2}$  with  $B$  in tesla. We shall examine some of the striking data on magnetotransport and show how we can obtain a consistent interpretation of what is observed.

At very low temperatures, the conductivity in the strongly localized regime is given by the variable range hopping<sup>4</sup> (VRH) formula,

$$\sigma = \sigma_0 \exp[-(T_0/T)^{1/\alpha}], \quad (1)$$

where the prefactor  $\sigma_0$  may depend slowly on  $T$  and the exponent  $\alpha$  is 4 (Mott's law) in the absence of interactions and 2 (Efros and Shklovskii's law) in the presence of Coulomb interactions.

For  $N_2$  doping concentrations up to 5%, activated or VRH conduction seem well established and no abnormal magnetoresistance is noted.<sup>5</sup> For  $N_2$  concentrations higher than 5%, Bhattacharyya<sup>5</sup> reported two regimes: for 10%  $N_2$ , the VRH regime for Mott's law shifts to lower temperatures (10 to 250 K) while the near room temperature (250 to 300 K) transport is a combination of band conduc-

tion and hopping. Still more recent work by Mares *et al.*<sup>6</sup> suggests activated conduction at room temperature. However, they reported a 9 meV activation energy at room temperature, when  $kT$  itself is 25 meV, and an Arrhenius fit will therefore not be unique. Furthermore, these authors appear to abandon the activation at lower temperatures in favor of a weak localization when interpreting the magnetoresistance. Thus a central issue is whether the localization is indeed weak.

Especially interesting is the 20% negative magnetoresistance below 4 K called "giant" in Ref. 6 where it is explained in terms of the Aharonov-Bohm effect seen in weakly localized metals, due to the de-enhancement of destructive coherent backscattering of the extended electron states. Such an explanation requires extended states at these low temperatures. In these polycrystalline samples, the required phase coherence for coherent backscattering demands a phase memory length  $L_\phi$  that is much bigger than  $d$ , and does not seem plausible for grains inhomogeneously embedded in an amorphous intergranular material.

For small magnetic fields, it is generally true that  $|\Delta R| \approx \beta B^2$ . This basic requirement follows from a combination of (i) a small field perturbative expansion and (ii) isotropic symmetry considerations, see Ref. 7. Regardless of the sign, the initial change in magnetoresistance versus  $B$  must always be quadratic, since the cyclotron radius  $\ell_B$  will be larger than other length scales for low  $B$ , implying that there can be no significant alteration to an initial ground state. The data for UNCD from Mares *et al.*<sup>6</sup> seem to show a small negative  $\beta$ . Unfortunately, our attempts to fit the data to weak localization theory had not been successful since the latter predicts a  $B^{5/2}$  law in three-dimensions (3D).<sup>8</sup> Weak localization theory is not the only plausible explanation for recent experimental data.<sup>6</sup> Quantum interference effects giving rise to a negative magnetoresistance in the VRH regime were predicted by Nguyen *et al.*<sup>9</sup> and subsequently reported by Tremblay *et al.*<sup>10</sup> in  $n$ -type GaAs structures.

We believe that we are always in the strongly localized regime for UNCD samples of the type.<sup>6</sup> First, it is hard to understand how one can have extended states at low tem-

<sup>a)</sup>Electronic mail: moo@um.es.

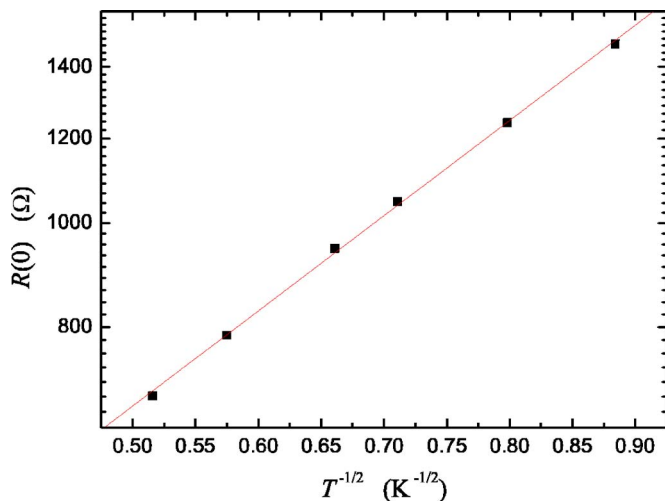


FIG. 1. (Color online) Resistance as a function of  $T^{-1/2}$  on semilogarithmic scale for a sample with 20% nitrogen concentration.

peratures and yet a variable range hopping mechanism at higher temperatures without some exotic phase transition perhaps. Second, a proper analysis of the previously reported results explicitly shows a VRH law in all instances. We have considered the zero field data in Fig. 2 of Ref. 6, which correspond to the resistance of a sample with 20%  $N_2$  concentration at various temperatures. In Fig. 1, we plot this resistance on a logarithmic scale as a function of  $T^{-1/2}$ , and we can see how the data follow an Efros and Shklovskii law rather well. Although the range of data available is small and hence other VRH model laws, such as  $T^{-1/4}$  cannot be ruled out, we can certainly conclude that it is a VRH-type mechanism. In fact, the data cannot be adjusted to a metallic behavior, which should be basically temperature independent.

What is also clear from the experimental results is that there is a strong change in the characteristic temperature  $T_0$  governing the VRH regime when the  $N_2$  concentration exceeds 5%. We believe that this may be due to an overlap of the two Hubbard subbands rather than a phase transition from the diffusive to the localized regime. At small concentrations, we have few impurities and their overlap is very small, so the impurity subbands are very narrow and do not overlap. All impurities are then singly occupied. When the concentration is close to 5%, the two subbands merge, and we have empty and doubly occupied impurities. The conduction mechanism still remains as VRH but with a characteristic temperature  $T_0$  much smaller due to the overlap of the two subbands.

Merging of the two Hubbard subbands also explains the reported variation of free spin numbers. When the two subbands do not overlap and all impurities are singly occupied, the density of free spins coincides with that of impurities. When the bands overlap and a proportion of the impurities is empty or doubly occupied, the ESR signal diminishes. This picture is in accord with the experimental data [see Fig 1(b)] of Ref. 5.

Now, we present numerical simulations in the strongly localized regime. Previously,<sup>11</sup> we found that the strongly localized regime is well described by the model of Nguyen *et al.*,<sup>9</sup> which consists in the directed path approximation of the Anderson model and a site disorder energy that can only take two values at random  $W$  or  $-W$ .

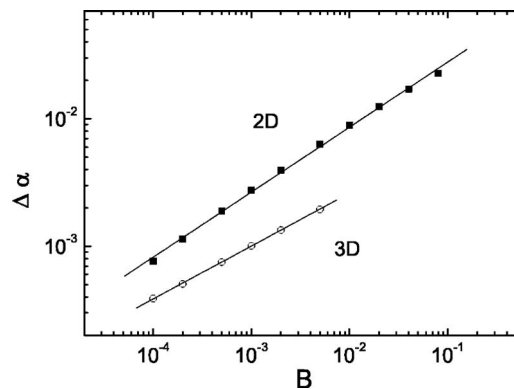


FIG. 2. Decrease in  $\xi(B)^{-1}$  as a function of  $B$  for 2D (squares) and 3D (circles) systems on a double logarithmic scale. The units of  $B$  are in flux quantum per plaquette and correspond to the same scale as in Fig. 3 for  $25 \text{ nm}^2$  plaquettes.

The assumption of directed paths makes it feasible to handle very large system sizes. To simplify the programming complexity in 3D systems, we have considered a bcc lattice with the vector joining the two terminal points along the direction  $(1,0,0)$ . In this way, we can propagate layer by layer, with each layer being a piece of a square lattice. We have also calculated two-dimensional (2D) samples with path lengths up to  $l=3200$  and 3D samples with  $l$  up to 1600 lattice spacings. We have averaged over  $10^6$  realizations in 2D systems and over  $2 \times 10^4$  realizations for the larger 3D systems.

The magnetic field is introduced through the Peierls phase of the transfer elements,  $te^{iA}$ , where  $A$  is the gauge potential. We can choose the gauge so that the potential is independent of one coordinate and proportional to the other  $A = \pm \gamma y/2$ , where  $\gamma = 2\pi\Phi/\Phi_0$  is the fractional flux per plaquette. We measure the magnetic field  $B$  in units of the elementary quantum flux  $\Phi_0 = h/2e$  per plaquette in the simulation.

The magnetic field effectively increases the localization length, and hence we have negative magnetoresistance. In Fig. 2, we represent the decrease in the inverse of the localization length  $\Delta = |\xi(B)^{-1} - \xi(0)^{-1}|$  as a function of  $B$  for 2D and 3D systems on a double logarithmic scale. The 2D data follow a straight line with slope 0.51, so the inverse of the localization length behaves as

$$\xi(B)^{-1} = \xi(0)^{-1} + a\sqrt{B}. \quad (2)$$

This behavior was already found by Medina and Kardar, see Ref. 12 and references cited therein. For values of the field lower than those shown in Fig. 2, the data tend to the  $B^2$  behavior predicted by the perturbation theory for very small fields. The data for 3D systems can also be fitted to a straight line, but with a smaller slope, roughly equal to 0.4.

If we assume that the main effect of the magnetic field is to change the localization length [Eq. (2)] without appreciably changing the density of states, we obtain general results valid for all types of VRH mechanisms. The dependence of the characteristic temperature in Eq. (1) on the localization length is determined by the exponent  $\alpha$ ,  $T_0 = c\xi^{1-\alpha}$ .<sup>4</sup> Inserting the field dependence of  $\xi$  from Eq. (2), and noting that the field term Eq. (2) is very small, we find

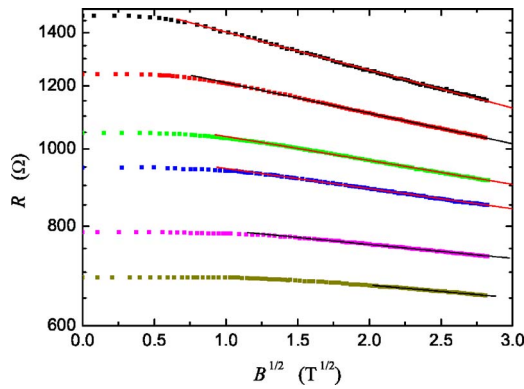


FIG. 3. (Color online) Magnetoresistance as a function of  $B^{1/2}$  for several temperatures of a sample with 20% nitrogen concentration. Note the logarithmic scale in the vertical axis.

$$\Delta \ln \sigma(B) \approx \left( \frac{T_0}{T} \right)^{1/\alpha} \frac{\alpha - 1}{\alpha} \xi(0) \alpha \sqrt{B}. \quad (3)$$

In our case,  $\alpha$  is close to 2, so the change in the logarithm of the conductance should be roughly proportional to  $\sqrt{B}/T$ .

In Fig. 3, we have plotted the resistance  $R$  in logarithmic scale as a function of  $\sqrt{B}$  from the magnetoresistance results of Mares *et al.*<sup>6</sup> for several temperatures (their original paper plotted  $R$  versus  $B$ ). We note how the data follow straight lines over a wide interval of the fields, in agreement with Eq. (3). For low values of the field ( $B < 1$  T), we see the perturbative regime, where the magnetoresistance is proportional to  $B^2$ , which smoothly joints our regime of interest.

We can further support the case for VRH conduction by studying the temperature dependence of the slopes of the straight lines in Fig. 3 as a function of  $T^{-1/2}$ . The VRH models imply a change in the logarithm of the magnetoconductance proportional to  $\sqrt{T_0}/T$ , as given by Eq. (3). We have checked that the previous slopes are proportional to  $T^{-1/2}$  in agreement with Eq. (3).

The crossover between the perturbative regime and the regime where the magnetoresistance goes as  $\sqrt{B}$  should take place when the magnetic length  $\ell_B$  is approximately equal to the typical hopping length at each  $T$ . We note in Fig. 3 how the linear regime starts at larger values of the field as  $T$

decreases and the hopping length increases. In order to be more quantitative, we have obtained the critical field  $B^*$  between the perturbative  $B^2$  and the  $\sqrt{B}$  regimes, similar to Mares *et al.*,<sup>6</sup> at the field for which the straight fitting line takes the experimental zero field value. Then,  $l_{\text{hop}} \approx \ell_B$ . We have checked that this length is proportional to  $T^{-1/2}$ , which is the expected dependence of the hopping length with temperature, in agreement with our VRH interpretation of the data. The values of the hopping length obtained in this way are quite reasonable for this material.

In the near future, we hope to extend our results to boron-doped diamond and study their possible implications on the important phenomena of superconductivity, recently observed in this material.<sup>13</sup>

Support from the Fundacion Seneca, Murcia, Project Nos. 03105/PI/05 and 04781/IV3/06, and from the DGI, Spain, Project No. FIS2006-11126 are gratefully acknowledged.

- <sup>1</sup>J. Pernot, C. Tavares, E. Gheeraert, E. Bustarret, M. Katagiri, and S. Koizumi, Appl. Phys. Lett. **89**, 122111 (2006).
- <sup>2</sup>A. M. Stoneham, Nat. Mater. **3**, 3 (2004).
- <sup>3</sup>M. D. Parr and D. K. Reinhard, Diamond Relat. Mater. **15**, 207 (2006).
- <sup>4</sup>N. F. Mott and E. A. Davis, *Electronic Processes in Non-Crystalline Materials*, 2nd ed. (Clarendon, Oxford, 1979).
- <sup>5</sup>S. Bhattacharyya, Phys. Rev. B **70**, 125412 (2004).
- <sup>6</sup>J. J. Mares, P. Hubik, J. Kristofik, D. Kindl, M. Fanta, M. Nesladek, O. Williams, and D. M. Gruen, Appl. Phys. Lett. **88**, 092107 (2006).
- <sup>7</sup>L. D. Landau, *Electrodynamics of a Continuous Media*, 2nd ed. (Pergamon, New York, 1984).
- <sup>8</sup>B. L. Altshuler, A. G. Aronov, and B. Z. Spivak, JETP Lett. **33**, 94 (1981).
- <sup>9</sup>V. L. Nguyen, B. Z. Spivak, and B. I. Shklovskii, Pis'ma Zh. Eksp. Teor. Fiz. **41**, 35 (1985) [JETP Lett. **41**, 42 (1985)]; Zh. Eksp. Teor. Fiz. **89**, 11 (1985). [Sov. Phys. JETP **62**, 1021 (1985)].
- <sup>10</sup>F. Tremblay, M. Pepper, R. Newbury, D. Ritchie, D. C. Peacock, J. E. F. Frost, G. A. C. Jones, and G. Hill, Phys. Rev. B **40**, 10052 (1989).
- <sup>11</sup>A. M. Somoza, M. Ortuño, and J. Prior, Phys. Rev. Lett. **99**, 116602 (2007); J. Prior, A. M. Somoza, and M. Ortuño, Phys. Rev. B **72**, 024206 (2005); Phys. Status Solidi B **243**, 395 (2006).
- <sup>12</sup>E. Medina and M. Kardar, Phys. Rev. B **46**, 9984 (1992).
- <sup>13</sup>M. Nesladek, D. Tromson, C. Mer, P. Bergonzo, P. Hubik, and J. J. Mares, Appl. Phys. Lett. **88**, 232111 (2006); J. J. Mares, M. Nesladek, P. Hubik, D. Kindl, and J. Kristofik, Diamond Relat. Mater. **16**, 1 (2007).